Reconstructing the archosaur radiation using a Middle Triassic archosauriform tooth assemblage from Tanzania (#39444)

First submission

Guidance from your Editor

Please submit by **8 Aug 2019** for the benefit of the authors (and your $200 publishing discount).

Structure and Criteria
Please read the 'Structure and Criteria' page for general guidance.

Raw data check
Review the raw data. Download from the materials page.

Image check
Check that figures and images have not been inappropriately manipulated.

Privacy reminder: If uploading an annotated PDF, remove identifiable information to remain anonymous.

Files
Download and review all files from the materials page.

8 Figure file(s)
3 Table file(s)
2 Raw data file(s)

Structure and Criteria

Structure your review

The review form is divided into 5 sections. Please consider these when composing your review:

1. **BASIC REPORTING**
2. **EXPERIMENTAL DESIGN**
3. **VALIDITY OF THE FINDINGS**
4. General comments
5. Confidential notes to the editor

You can also annotate this PDF and upload it as part of your review

When ready submit online.

Editorial Criteria

Use these criteria points to structure your review. The full detailed editorial criteria is on your guidance page.

BASIC REPORTING

- Clear, unambiguous, professional English language used throughout.
- Intro & background to show context. Literature well referenced & relevant.
- Structure conforms to PeerJ standards, discipline norm, or improved for clarity.
- Figures are relevant, high quality, well labelled & described.
- Raw data supplied (see PeerJ policy).

EXPERIMENTAL DESIGN

- Original primary research within Scope of the journal.
- Research question well defined, relevant & meaningful. It is stated how the research fills an identified knowledge gap.
- Rigorous investigation performed to a high technical & ethical standard.
- Methods described with sufficient detail & information to replicate.

VALIDITY OF THE FINDINGS

- Impact and novelty not assessed. Negative/inconclusive results accepted. *Meaningful* replication encouraged where rationale & benefit to literature is clearly stated.
- All underlying data have been provided; they are robust, statistically sound, & controlled.
- Speculation is welcome, but should be identified as such.
- Conclusions are well stated, linked to original research question & limited to supporting results.

Standout reviewing tips

The best reviewers use these techniques

Tip	*Example*
Support criticisms with evidence from the text or from other sources	*Smith et al (J of Methodology, 2005, V3, pp 123) have shown that the analysis you use in Lines 241-250 is not the most appropriate for this situation. Please explain why you used this method.*
Give specific suggestions on how to improve the manuscript	*Your introduction needs more detail. I suggest that you improve the description at lines 57- 86 to provide more justification for your study (specifically, you should expand upon the knowledge gap being filled).*
Comment on language and grammar issues	*The English language should be improved to ensure that an international audience can clearly understand your text. Some examples where the language could be improved include lines 23, 77, 121, 128 – the current phrasing makes comprehension difficult.*
Organize by importance of the issues, and number your points	*1. Your most important issue* *2. The next most important item* *3. …* *4. The least important points*
Please provide constructive criticism, and avoid personal opinions	*I thank you for providing the raw data, however your supplemental files need more descriptive metadata identifiers to be useful to future readers. Although your results are compelling, the data analysis should be improved in the following ways: AA, BB, CC*
Comment on strengths (as well as weaknesses) of the manuscript	*I commend the authors for their extensive data set, compiled over many years of detailed fieldwork. In addition, the manuscript is clearly written in professional, unambiguous language. If there is a weakness, it is in the statistical analysis (as I have noted above) which should be improved upon before Acceptance.*

Reconstructing the archosaur radiation using a Middle Triassic archosauriform tooth assemblage from Tanzania

Devin K Hoffman [Corresp., 1], **Hunter Edwards** [1, 2], **Paul M Barrett** [3], **Sterling J Nesbitt** [1]

[1] Department of Geosciences, Virginia Polytechnic Institute and State University (Virginia Tech), Blacksburg, Virginia, United States of America

[2] Department of Geological Sciences, University of Cape Town, Rondebosch, South Africa

[3] Department of Earth Sciences, Natural History Museum, London, United Kingdom

Corresponding Author: Devin K Hoffman
Email address: devinkh5@vt.edu

Following the Permo-Triassic mass extinction, Archosauriformes – the clade that includes crocodylians, birds, and their extinct relatives – rapidly diversified into numerous distinct lineages, became distributed globally, and, by the Late Triassic, filled a wide array of resource zones. Current scenarios of archosauriform evolution are ambiguous with respect to whether their taxonomic diversification in the Early–Middle Triassic coincided with the initial evolution of dietary specializations that were present by the Late Triassic, or if their ecological disparity arose sometime after lineage diversification. Late Triassic archosauriform dietary specialization is recorded by morphological divergence from the plesiomorphic archosauriform tooth condition (laterally-compressed crowns with serrated carinae and a generally triangular lateral profile). Unfortunately, the roots of this diversification are poorly documented, with few known Early–Middle Triassic tooth assemblages, limiting characterizations of morphological diversity during this critical, early period in archosaur evolution. Recent fieldwork (2007–2017) in the Middle Triassic Manda Beds of the Ruhuhu Basin, Tanzania, recovered a tooth assemblage that provides a window into this poorly sampled interval. To investigate the taxonomic composition of that collection, we built a dataset of continuous quantitative and discrete morphological characters based on *in situ* teeth of known taxonomic status (e.g., *Nundasuchus*, *Parringtonia*: N = 65) and a sample of isolated teeth (N = 31). Using crown heights from known taxa to predict tooth base ratio (= base length/base width), we created a quantitative morphospace for the tooth assemblage. The majority of isolated, unassigned teeth fall within a region of morphospace shared by several Manda taxa (e.g., *Nundasuchus*, *Parringtonia*); two isolated teeth fall exclusively within a '*Pallisteria*' morphospace. A non-metric multidimensional scaling ordination (N = 67) of 11 binary characters reduced overlap between species. The majority of the isolated teeth from the Manda assemblage fall within the *Nundasuchus* morphospace. This indicates these teeth

are plesiomorphic for archosauriforms as *Nundasuchus* exhibits the predicted plesiomorphic condition of archosauriform teeth. Our model shows that even the conservative tooth morphologies of archosauriforms can be differentiated and assigned to species/genus level, rendering the model useful for identifying isolated teeth. The large overlap in tooth shape among the species present and their overall similarity indicates that dietary specialization lagged behind species diversification in archosauriforms from the Manda Beds, a pattern predicted by Simpson's 'adaptive zones' model. Although applied to a single geographic region, our methods offer a promising means to reconstruct ecological radiations and are readily transferable across a broad range of vertebrate taxa throughout Earth history.

Reconstructing the Archosaur Radiation using a Middle Triassic Archosauriform Tooth Assemblage from Tanzania

Devin K. Hoffman[1], Hunter Edwards[1,2], Paul M. Barrett[3], Sterling J. Nesbitt[1]
[1] Department of Geosciences, Virginia Tech, Blacksburg, VA, USA
[2] Department of Geological Sciences, University of Cape Town, Rondebosch 7701, South Africa
[3] Department of Earth Sciences, Natural History Museum, London, UK

Corresponding Author:
Devin K. Hoffman[1]
926 West Campus Drive, Blacksburg, VA, 24061, USA
Email address: devinkh5@vt.edu

Following the Permo-Triassic mass extinction, Archosauriformes – the clade that includes crocodylians, birds, and their extinct relatives – rapidly diversified into numerous distinct lineages, became distributed globally, and, by the Late Triassic, filled a wide array of resource zones. Current scenarios of archosauriform evolution are ambiguous with respect to whether their taxonomic diversification in the Early–Middle Triassic coincided with the initial evolution of dietary specializations that were present by the Late Triassic, or if their ecological disparity arose sometime after lineage diversification. Late Triassic archosauriform dietary specialization is recorded by morphological divergence from the plesiomorphic archosauriform tooth condition (laterally-compressed crowns with serrated carinae and a generally triangular lateral profile). Unfortunately, the roots of this diversification are poorly documented, with few known Early–Middle Triassic tooth assemblages, limiting characterizations of morphological diversity during this critical, early period in archosaur evolution. Recent fieldwork (2007–2017) in the Middle Triassic Manda Beds of the Ruhuhu Basin, Tanzania, recovered a tooth assemblage that provides a window into this poorly sampled interval. To investigate the taxonomic composition of that collection, we built a dataset of continuous quantitative and discrete morphological characters based on *in situ* teeth of known taxonomic status (e.g., *Nundasuchus*, *Parringtonia*: N = 65) and a sample of isolated teeth (N = 31). Using crown heights from known taxa to predict tooth base ratio (= base length/base width), we created a quantitative morphospace for the tooth assemblage. The majority of isolated, unassigned teeth fall within a region of morphospace shared by several Manda taxa (e.g., *Nundasuchus*, *Parringtonia*); two isolated teeth fall exclusively within a '*Pallisteria*' morphospace. A non-metric multidimensional scaling ordination (N = 67) of 11 binary characters reduced overlap between species. The majority of the isolated teeth from the Manda assemblage fall within the *Nundasuchus* morphospace. This

indicates these teeth are plesiomorphic for archosauriforms as *Nundasuchus* exhibits the predicted plesiomorphic condition of archosauriform teeth. Our model shows that even the conservative tooth morphologies of archosauriforms can be differentiated and assigned to species/genus level, rendering the model useful for identifying isolated teeth. The large overlap in tooth shape among the species present and their overall similarity indicates that dietary specialization lagged behind species diversification in archosauriforms from the Manda Beds, a pattern predicted by Simpson's 'adaptive zones' model. Although applied to a single geographic region, our methods offer a promising means to reconstruct ecological radiations and are readily transferable across a broad range of vertebrate taxa throughout Earth history.

Introduction

Adaptive radiations, or evolutionary diversifications, play a critical role in the history of life as clades speciate and fill new ecological roles over geologically rapid time intervals (Simpson, 1944; Schluter, 1996). Although there are examples of adaptive radiations that are not speciose (e.g. Darwin's finches), or adaptively disparate (e.g. crotaphytine and oplurine iguanids), such a framework is still useful for structuring macroevolutionary questions and explaining present (and past) biological diversity (Gavrilets and Losos, 2009). Adaptive radiations and the shifts in evolutionary rates associated with them are among the most studied aspects of evolutionary biology (e.g. Stanley, 1979; Losos and Miles, 1994, 2002; Gavrilets and Losos, 2009; Revell et al., 2018; Slater and Friscia, 2019). However, empirical uncertainties remain regarding many of the properties of adaptive radiations (Gavrilets and Losos, 2009; Slater and Friscia, 2019), with the relative timings of lineage diversification and ecological disparity during adaptive radiations being one such problem. Does lineage diversification come first, followed by specialization and evolution within an 'adaptive zone' (Simpson, 1944, 1953) or does ecological specialization drive lineage diversification simultaneously (Schluter, 1996)? In the former case species fill the same resource zones using similar, ancestral morphological structures (e.g. identical tooth morphologies), whereas in the latter each species would be expected to have a unique, derived morphology for its resource zone at the start of the radiation (for an empirical example, see Slater and Friscia, 2019). Determining which of these competing hypotheses operated in a particular case requires us to reconstruct an evolutionary radiation where a species-poor, adaptively constrained clade diversifies into a species-rich, adaptively disparate clade.

One such radiation occurred dur~~in~~g the Triassic Period, following the Permo-Triassic mass extinction (PTME: Raup, 1979; Erwin, 1994; Chen and Benton, 2012; Benton and Newell,

2014) as archosauriforms recovered, rapidly diversified, and spread across Pangea to dominate terrestrial ecosystems for the next 150 million years (Nesbitt, 2011; Ezcurra and Butler, 2018). In addition to Archosauriformes being a speciose and disparate radiation, they also provide an opportunity to test adaptive radiations at a higher phylogenetic level. Lineage diversification of archosaurs was rapid after the PTME, and by the Middle Triassic many non-archosaurian archosauriform and crown archosaur clades had appeared (Ezcurra, 2016; Foth et al., 2016; Ezcurra and Butler, 2018). By the Late Triassic archosaurs filled a wide variety of ecological roles, from top predators to large herbivores, and were represented in terrestrial, freshwater, and even marine ecosystems (e.g. Li et al., 2006; Butler et al., 2019). If lineage diversification occurs first, followed by subsequent ecological disparity, we would expect Middle Triassic archosauriforms from across the tree to present a limited range of ecologies. The question that arises is how best to measure ecological disparity? Ecological disparity covers a variety of physiological, behavioral, and morphological traits but the nature of the fossil record limits its measure primarily to morphology. Previous work has used cranial morphology as a measure of disparity (e.g. Foth et al., 2016); however complete, or even partial, skulls are rare for Early–Middle Triassic archosauriforms. Therefore, an alternative morphological system to approximate ecological disparity is needed. In this study we use teeth as an indicator of ecological disparity because they have relatively high preservation potential (e.g. Turner-Walker, 2008) and offer a direct link to ecology through diet (Lucas, 1979; Dessem, 1985; Scallon and Shine, 1988; Sander, 1997; Linde, Palmer & Gómez-Zurita, 2004; Santana, Strait & Dumont, 2011; Zahradnicek et al., 2014). We consider diet as the aspect of ecology of interest for both the relative ease of inference from morphology alone and the use of diet in previous studies of evolutionary radiations (e.g. Slater and Friscia, 2019).

Although tooth assemblages are rare in Middle Triassic terrestrial settings, recent fieldwork (2007, 2008, 2012, 2015, 2017) in the Manda Beds of the Ruhuhu Basin, Tanzania (Sidor and Nesbitt, 2017), has revealed a rich assemblage of archosauriforms known from postcrania and partial crania, including teeth (e.g. Nesbitt et al., 2010; 2014; Smith et al., 2018). Specifically, these teeth come from the middle and upper Lifua Member bone accumulations (Smith et al., 2018), which are thought to be Anisian in age (Rubidge, 2005) but may be as young as early Carnian (Ottone et al., 2014; Marsicano et al., 2016; Wynd et al., 2018; Peecook et al., 2018). If the Anisian age is correct, then this is one of the oldest, diverse archosaur faunas known that is also represented by specimens from historical collections (e.g. Butler et al., 2009; 2017; Nesbitt et al., 2010; 2013; 2014; 2017; Barrett, Nesbitt & Peecook, 2015). Using a combination of information from these new and historical collections, we quantify tooth disparity in this earliest part of the archosaur radiation to generate a morphospace visualization. From this we can assign isolated teeth to specific taxon, visualize inter- and intraspecific variation as well as intra-individual variation, and use this variation as a window into the ecological disparity of the archosauriforms within the Lifua Member assemblage. To achieve these goals we use a combination of *in situ* teeth from jaw elements assignable to particular species (Figure 1), and isolated teeth attributable to Archosauriformes (Figure 2). Of particular interest is whether the isolated teeth fall within, or expand, the region of morphospace occupied by the described Manda Beds taxa.

Institutional Abbreviations – **NHMUK**, Natural History Museum, London, U.K.; **NMT**, National Museum of Tanzania, Dar es Salaam, Tanzania.

Materials & Methods

The 31 isolated teeth included in this study were ~~all~~ collected from surface accumulations ~~of vertebrate fossils~~ during fieldwork in 2007, 2008, 2012, 2015, and 2017 from the Manda Beds of the Ruhuhu Basin by a multi-institutional team (Sidor and Nesbitt, 2017). All of the isolated teeth included in this study are currently housed at Virginia Tech Department of Geosciences and will be permanently reposited and managed in the National Museum of Tanzania. In addition to these isolated teeth (seven of which were referred to *Nundasuchus*: see Nesbitt et al., 2014), we also included teeth from within the tooth-bearing elements of five taxonomically distinct archosauriforms from the Manda Beds: *Nundasuchus* (NMT RB48), *Parringtonia* (NMT RB426), *Asilisaurus* (NMT RB837), '*Pallisteria*' (NHMUK PV R36620), and one currently undescribed pseudosuchian that we refer to ~~–~~by its specimen number (NMT RB187). We assign the isolated teeth to Archosauriformes on the basis of their serration morphology (Nesbitt, 2011) as well as their general ziphodont construction, including lateral compression (e.g. Godefroit and Cuny, 1997).

To quantify tooth shape, linear measurements (total crown height, base width, and fore-aft base length) and denticle counts were made following the protocol in Smith, Vann & Dodson (2005), although due to the smaller size of the teeth in our study, we used 1 mm denticle densities, rather than 5 mm densities (Supplementa1 Data S1). All statistical analyses were performed in R (v 3.1.2) and the RStudio console (v 1.1.383). All graphs of quantitative data were made using the R package "ggplot2" (Wickham, 2009). To capture tooth disparity (from log-transformed linear measurements) we used sum of variances with 95% predictive intervals following the methodology of Larson, Brown & Evans (2016). We chose to use sum of variances as our measure of disparity due to its prevalence in the literature and its robustness when working with small sample sizes. Sample size varied from 2–14 teeth, however, sample size does

not significantly affect the sum of variance analysis (Ciampaglio, Kemp, & McShea, 2001). In *Asilisaurus* the 14 teeth largely contributed base and width measurements because only three teeth were complete enough to measure crown height. We constructed a linear model in R predicting the variable of tooth base shape (ratio of mesiodistal length over labiolingual width) by the variables of total crown height and species-level assignment such that base shape = total crown height * species assignment. The effects of each species on predicting tooth base shape were elucidated using the R package "lsmeans" (Lenth, 2016) using a pairwise comparison in the model by taxon. We plotted the teeth of known taxonomic affinity using ggplot2 (Wickham, 2009) to produce a base morphospace into which we plotted results from the isolated teeth for comparison.

Simple quantitative measurements only capture the overall shape of the teeth, and all of the teeth in the study resemble the hypothetical ancestral archosauriform tooth (serrated, recurved, and laterally compressed: Nesbitt, 2011). In order to more fully capture and describe the subtle variation of these teeth, a method of capturing discrete variation is needed. Non-metric multidimensional scaling (NMDS) is an ordination method that visualizes variation that can incorporate discrete qualitative features. We created a set of 11 binary characters for scoring isolated and *in situ* teeth for NMDS (Table 1, Figure 3, Supplementa1 Data S2). All characters except one are new to this analysis (trait 6, dental caudae = shallow grooves extending from between two adjacent denticles present/absent is taken from Abler [1992]). None of the traits used in this study have been used in phylogenetic analyses of archosauriforms, in order to avoid circular reasoning when comparing our ecological signal to taxonomic and clade identity. The NMDS analysis was conducted in PAST (Hammer, Harper & Ryan, 2001) with a Bray-Curtis transformation. We ran an additional NMDS analysis in PAST using average taxon and

morphotype scores where traits were scored for each taxon with >50% agreement of *in situ* teeth. Traits for which <50% of the specimens in the taxon or morphotype were scored as unknown ("?").

Isolated Tooth Descriptions

Morphotype A: These teeth (Figure 2A) are generally triangular in outline in lateral view and most are recurved (the point of the crown is distal to the distal-most extent of the crown base) although the remainder have crown tips that are level with the distal-most extent of the crown base. The labial and lingual sides of the crown lack ridges (i.e. no fluting), and the labial side of the crown exhibits greater convexity than the lingual side. The mesial denticle series terminates more apically along the crown margin than the distal series, which continues along the entire height of the crown though both start at the tip of the crown. The mesial denticle series is also offset from the mesial-distal long axis of the crown base, deflecting to the lingual side toward the crown base. The denticle densities range from 2–5 per mm. Denticle caudae (Abler, 1992), which are shallow grooves extending from between two adjacent denticles, are often present and directed parallel to the denticles. These denticle caudae are most easily viewed in mesial or distal view (Figure 3F).

In general, Morphotype A teeth strongly resemble both *in situ* and isolated teeth of *Nundasuchus* (Figure 1; Nesbitt et al., 2014). Particularly important features are the presence of denticle caudae, an unequal labial-lingual curvature, and the more apical termination of the mesial denticle series relative to the distal denticle series. Also like *Nundasuchus*, teeth of Morphotype A exhibit a mix of states in the changing curvature of the mesial crown edge in lateral view, with some teeth gradually changing angles and others exhibiting an abrupt shift in

angle. The *in situ* teeth of *Nundasuchus* can exhibit either state depending on the proximity of the mesial edge of the crown to the distal edge of the preceding tooth. Though this combination of traits is only found in *Nundasuchus* in the Manda Beds fauna, archosauriforms from the Middle and Upper Triassic elsewhere (e.g. de Oliveira and Pinheiro, 2017; Schoch et al., 2018).

Morphotype B: These teeth (Figure 2B) are triangular in shape in lateral view and are occasionally recurved, although in most the apical tip of the crown is approximately level with the distal-most end of the crown base. Morphotype B tooth crowns lack fluting and, in contrast to Morphotype A, the labial and lingual curvatures are equal. None of the teeth are bulbous (no labiolingual measurements are greater than crown base width). In the majority of Morphotype B teeth the mesial margin of the crown possesses a single point where the angle of the mesial carina changes abruptly. As in Morphotype A teeth, the mesial series of denticles in Morphotype B teeth terminates on the crown further apically than the distal series, which often terminates at the crown base. However, the mesial row of denticles is in line with the mesial-distal long axis of the crown base. The denticle densities range from 3–8 per mm. Denticle caudae are present on some of the teeth and are directed parallel to the denticles. Although these teeth bear a strong resemblance to Morphotype A, they can be differentiated by their equal labial and lingual curvatures. Morphotype B teeth are similar to some of the *in situ* and isolated *Nundascuhus* teeth (Figure 1,2; Nesbitt et al., 2014).

Morphotype C: This morphotype (Figure 2C) is represented by a single tooth in our assemblage, NMT RB831. The overall shape is tall, near conical, and recurved. The crown lacks fluting and the labial curvature is greater than the lingual curvature. Although its labial-lingual curvature is unequal, the mesial denticle series is positioned along the midline of the mesial-distal long axis. The orientation of the mesial edge of the tooth changes gradually, forming a long, continuous

curve. The tooth is not bulbous. Denticle densities range from 2–4 per mm, and no denticle caudae are present. There is no variation in either the shape or size of the denticles between the mesial and distal series or along the length of the crown. Unlike either Morphotypes A or B, the mesial series of denticles in Morphotype C ends at approximately the same level on the crown as the distal series, just above the crown base.

In general size and shape, as well as in many of its discrete features, the Morphotype C tooth is similar to the teeth of '*Pallisteria*' based on our observations. The teeth of the latter taxon are large, conical, recurved, and possess unequal labial-lingual curvature. The denticle density is low (< 3 per mm) in the middle part of the tooth crown and denticles show little variation in shape or size. Unfortunately, none of the '*Pallisteria*' teeth could be scored for Trait 7 (termination height of the mesial denticle series; Table 1) due to poor preservation of the denticles, which otherwise differentiates Morphotype C teeth from morphotypes A and B. If Morphotype C is similar to, or is, '*Pallisteria*', then subsequent '*Pallisteria*' tooth discoveries should be expected to have sub-equally extending mesial and distal denticle rows.

In situ **Tooth Descriptions**

Nundasuchus: We included a total of 13 *Nundasuchus* teeth, six *in situ* and seven isolated, originally described in Nesbitt et al. (2014). The teeth range in height from 5.6 to 22 mm with denticle densities from 2–5 per mm. All the teeth are labio-lingually compressed and are serrated on both mesial and distal margins. Only one tooth possesses a recurved tip that extends past the distal-most end on the tooth base. Most teeth are smooth on the sides with a single exception exhibiting fluting. All of the teeth possess: unequal labial-lingual curvatures, a mesial row of denticles that terminates higher on the tooth crown than the distal row of denticles, and a mesial

carina that is offset from the midline. Only two of the teeth possess dental caudae and one tooth is bulbous. In some teeth the mesial and distal denticle rows differ in size and/or in shape. About half the teeth have a distinct point on the mesial margin where the angle of the edge changes abruptly. For the *in situ* teeth this seems to be related to how close the tooth is to the preceding socket, with the closer the distance being associated with an abrupt angle shift point.

Asilisaurus: We included 14 *in situ* teeth though only three of these included more than the very base of the tooth. These three ranged in height from 1.6 to 2.9 mm and had a denticle density of ~8 per mm. The teeth are closely packed, ankylosed to the sockets, and peg-like in shape (Nesbitt et al., 2010). All of the teeth have: smooth sides, equal labial-lingual curvature, and subeven mesial and distal row of denticles. None of the *Asilisaurus* teeth possess dental caudae and the mesial edge of the teeth changes angles gradually.

Parringtonia: Of the 14 teeth in the study, 12 were *in situ* and the other two larger, isolated teeth. The teeth range in size from 2.5–21.6 mm, though the tallest *in situ* tooth is 8.3 mm, and the denticle densities vary from 5–15 per mm. Most of the *Parringtonia* teeth lacked crown tips, though the two complete teeth are not recurved. All of the teeth are labio-lingually compressed and possess fluting and a mesial carina along the midline. The mesial and distal denticle series of all the teeth remain constant in both shape and size, though the mesial denticle series terminates higher on the crown than the distal series. In all the teeth the mesial edge angle changes gradually.

NMT RB187: All 13 teeth of the teeth included from NMT RB187 are *in situ*. The labio-lingually compressed teeth range from 5.3–13.4 mm tall with denticle densities of 8–14 per mm. All of the teeth are recurved, fluted, and lack dental caudae. The mesial edge of the teeth changes gradually and follows the mesial-distal long axis. In teeth with preserved crown tips the shape of

the denticles remains constant. Of all the taxa included here, NMT RB187 exhibits the greatest degree of recurvedness.

'*Pallisteria*': We included 11 *in situ* teeth from the left and right maxillae of '*Pallisteria*'. These teeth are the largest of all the taxa, ranging from 36.1–70.3 mm, and have the lowest density, from 2–3 per mm. All except one are recurved and all have smooth crowns and lack dental caudae. Most of the teeth have uneven labial-lingual curvature and a mesial edge that changes angles gradually. The mesial carina is offset from the mesiodistal long axis in most the teeth and the denticles remains constant in shape and size along the height of the crown.

Results

For our linear model we predicted the tooth base shape (ratio of labiolingual base width to mesiodistal base length) using the total apicobasal crown height and the taxonomic affinity of the tooth (base ~ tch + taxon) with the lm() command in base R (Table 2). We found that tooth height was not a significant predictor of base shape ($p = 0.0933$. We used the R package "lsmeans" to further investigate the differences between the species' tooth shape (Table 3). From this metric NMT RB187 has a significantly higher base shape ratio than all other taxa except *Parringtonia* ($p = 0.3788$).

The sum of variances analysis (Figure 4) included all known Manda Beds archosauriform taxa with associated dentition and two of the three morphotypes, as only a single tooth of Morphotype C is present in our assemblage. These variances provide a quantification of intraspecific variation in tooth size and shape, and allow for an equal interspecific comparison. Mean variances ranged from a low of 0.02 log units in '*Pallisteria*', two large isolated teeth of *Parringtonia*, and Morphotype B, to a high of 0.145 log units in Morphotype A (Figure 4).

More useful for visualizing variation than the linear model and lsmeans contrasts are morphospace plots of the teeth from our generically determinate specimens, with the isolated, unidentified teeth added for comparison. There is much overlap in morphospace occupancy, particularly on the left side (shorter height) portion of the graph, although *'Pallisteria'* occupies its own section of morphospace in taller crown heights (Figure 5). Teeth towards the bottom of the morphospace (lower base ratio) are more rounded and cone-like, whereas those with higher base ratios are more laterally compressed. With size alone two of the Morphotype A teeth fall in '*Pallisteria'* morphospace and the Morphotype C tooth with *Nundasuchus* morphospace contrary to the discrete descriptive predictions. The relationship between base width and mesiodistal base length provides little more distinction of the taxa included, and the impact of crown size is still evident (Figure 6). In general the ratio of base mesiodistal length and labiolingual width follows a linear trend controlled by size.

A total of 21 isolated teeth and 46 *in situ* teeth of known affinity were complete enough to be scored for the NMDS analysis. Convex hulls are more differentiated than in the quantitative morphospace, with almost no overlap of *Nundasuchus* with either NMT RB187 or *Parringtonia* (Figure 7). Overlap of NMT RB187 and *Parringtonia* remains, but most of the isolated teeth fall exclusively within or adjacent to the zone of *Nundasuchus* and '*Pallisteria*' (Figure 7). The high degree of overlap between *Parringtonia* and NMT RB187 likely reflects their often-shared feature of having parallel ridges (fluting) along the labial and lingual sides of the tooth crown. The only other tooth in the study with fluting is a single example referred to *Nundasuchus*. The use of taxa and morphotype 'averages' in traits reveals similar groupings to the complete dataset, with average morphotype scores between those of known taxa (Figure 8).

297 **Discussion**

298 We present the first quantitative description of a Middle Triassic archosauriform tooth
299 assemblage, which reveals substantial conservation of tooth morphology at the beginning of the
300 archosaur radiation. Intraspecific variation appears to be as great, if not greater, than interspecific
301 variation. Morphotype A displays the greatest variance in tooth size in the sample, although
302 *Nundasuchus* has a very similar sum of variance structure (Figure 4). Driving at least part of the
303 pattern we see in our disparity analysis is whether more than a single individual of a given taxon
304 is included in our study. For example, NMT RB187, '*Pallisteria*', and *Parringtonia* all display
305 low disparity, but our sample includes only elements from a single individual of each taxon,
306 whereas the *Nundasuchus* sample includes *in situ* teeth from one lower jaw (the holotype
307 specimen) and associated isolated teeth assigned to the holotype (Figure 4). Although two of the
308 isolated teeth from our assemblage fall exclusively within the '*Pallisteria*' quantitative
309 morphospace, most of the isolated teeth fall within a zone of overlap between *Nundasuchus*,
310 NMT RB187, and *Parringtonia* (Figure 5). Much of this quantitative variation reflects body size
311 (Figure 6). *Nundasuchus* and '*Pallisteria*' are much larger than the other taxa, which helps to
312 differentiate their morphospace from that of smaller-bodied taxa. *Asilisaurus* is the smallest
313 taxon in our sample, but there is postcranial evidence of a larger silesaurid in the Lifua
314 assemblage (possibly a very large individual of *Asilisaurus*; Barrett, Nesbitt, & Peecook, 2015)
315 that would be comparable in size to *Nundasuchus* and '*Pallisteria*'. Recovery of teeth from
316 silesaurid individuals of this larger size might reduce some of the differentiation between them,
317 *Nundasuchus*, and '*Pallisteria*' though we would still expect silesaurid teeth to be smaller
318 relative to the same body size.

The NMDS ordination improves the differentiation of taxa, with *Asilisaurus* and the large-bodied predator '*Pallisteria*' more clearly separated from the still overlapping undescribed pseudosuchian, and *Parringtonia* and *Nundasuchus* exhibiting wide variation in morphospace overall, bridging the space between all taxa, and overlapping a substantial part of '*Pallisteria*' morphospace (Figure 7). These results identify two general areas of morphospace, one shared by the undescribed pseudosuchian and *Parringtonia* and the other by *Nundasuchus* and '*Pallisteria*'. The teeth of *Parringtonia* and the undescribed pseudosuchian share several features, notably presence of fluting, a mesial carina along the midline tooth axis, and a high denticle density (≥ 3 per mm). By contrast, *Nundasuchus* and '*Pallisteria*' teeth lack fluting, possess an offset mesial carina, unequal labial/lingual curvature, and have a low denticle density (< 3 per mm). This result is further supported when the average or typical score of each taxon is used, with NMT RB187, *Asilisaurus*, and *Parringtonia* clustering together versus *Nundasuchus* and '*Pallisteria*' on the other side of morphospace (Figure 8). Given that many of the isolated teeth resemble those of *Nundasuchus*, it is not surprising that most of the isolated teeth fall within the convex hull defined by *Nundasuchus* (Figure 7). We cannot, however, definitely assign these teeth to *Nundasuchus* due to the overlap in discrete characters among our included taxa.

Our results using both methods demonstrate that many of the isolated teeth resemble those from currently recognized taxa. However, several teeth fall outside of the morphospace defined by known taxa and could indicate either intraspecific variation (due to heterodonty or ontogeny) or could represent other, as yet unsampled, taxa. Our methodologies are flexible and the datasets can incorporate additional specimens as they are excavated, so these approaches

could be applied to other tooth assemblages throughout the Triassic across a broad range of spatial, temporal, and taxonomic scales.

Ecological Differentiation. There are some hints of dietary separation between large- and small-bodied archosaurs based on minor changes in tooth morphology and consideration of body size. However, our results, which show high degrees of overlap in tooth morphology suggest that ecological differentiation, at least in diet, appears to lag behind lineage diversification, at least with respect to Manda archosauriforms. Four of the five recognized taxa included here possess ziphodont dentitions (=labiolingual narrow crown [labiolingual width < 60% of mesiodistal length], recurved, typically serrated carinae, and no constriction at the cervix *sensu* Hendrickx, Mateus & Araújo, 2015) indicative of a carnivorous diet. Only *Asilisaurus* differs in possessing a conidont dentiton (=conical crowns with small denticles or no denticles, and typically fluted *sensu* Hendrickx, Mateus & Araújo, 2015). Conidonty is present in spinosaurids, many crocodylians, marine reptiles, and pterosaurs (Hendrickx, Mateus & Araújo, 2015) and has been linked to piscivory. Following this criterion *Asilisaurus* would be categorized as a potential piscivore. However, dietary reconstructions of *Silesaurus opolensis*, another silesaurid possessing similar dentition to *Asilisaurus*, have been herbivorous or omnivorous based upon dental microwear (Kubo and Kubo, 2014) or insectivorous based upon coprolites (Qvarnström et al., 2019). Thus, in the Manda Beds tooth assemblage there are two large-bodied carnivores (*Nundasuchus* and '*Pallisteria*'), two small-bodied carnivores (*Parringtonia* and an undescribed pseudosuchian), and one small-bodied, non-carnivore (*Asilisaurus*). The Middle Triassic Manda Beds may, therefore, be capturing the beginning of the 'Explosive Phase' of Simpson's (1944) theoretical model as lineages split and begin to move towards new adaptive zones. Further tooth assemblages will need to be evaluated to see if this is a broader trend that

holds across the Triassic archosaur radiation. We posit that the qualitative NMDS ordination method gives us the necessary lens for testing this hypothesis.

Conclusions

Simple quantitative measures of tooth shape were of limited use in characterizing the Middle Triassic Manda Beds archosauriform tooth assemblage because of the highly conserved morphology of many specimens. Instead, an ordination based on discrete characters provided a more effective means of differentiating the teeth of distinct taxa. Nevertheless, we found little evidence for significant ecological differentiation of tooth shape between the five taxa included in our study. Most isolated teeth (n = 17/21) fall within the spectrum of recognized taxon variation, and the remainder represent either unsampled taxa or unsampled intraspecific variation.

Our relatively simple metrics can be used to describe subtle differences in tooth morphology. These objective methods for grouping teeth provide a complimentary method for assigning teeth to dietary roles, a practice that typically relies on qualitative comparisons to the teeth of extant taxa of known diet (e.g. Fraser and Walkden, 1983; Sander, 1999; Barrett, 2000; Hungerbühler, 2000) or other fossil taxa (e.g. Dzik, 2003; Hendrickx, Mateus & Araújo, 2015; de Oliveira and Pinheiro, 2017). Furthermore, the methods applied herein provide an evaluation of ecological disparity that is separate from the features used in phylogenetic analyses, so that we can compare these two evolutionary phenomena independently. This method is readily transferable to tooth assemblages from other localities pertaining to any vertebrate clade. Our next step will be to apply this technique to richer Middle Triassic sites, as well as Late Triassic

386 sites, to understand how morphological and ecological diversity changed during the early stages
387 of the archosaur radiation.
388
389 **Acknowledgments**
390 We thank Dr. Kate Langwig and Dr. Josef Uyeda for their assistance and advice with R Studio,
391 and the Virginia Tech Paleobiology Research Group for helpful comments.

392 **Works Cited**

393 Abler, W. L., 1992, The serrated teeth of tyrannosaurid dinosaurs, and biting structures in other
394 animals: Paleobiology, v. 18, no. 2, p. 161-183.
395 Barrett, P. M., 2000, Prosauropods and iguanas: speculation on the diets of extinct reptiles. In
396 Sues HD, ed. *Evolution of Herbivory in Terrestrial Vertebrates: Perspectives from the*
397 *Fossil Record*. Cambridge: Cambridge University Press, 42-78.
398 Barrett, P. M., Nesbitt, S. J., and Peecook, B. R., 2015, A large-bodied silesaurid from the Lifua
399 Member of the Manda beds (Middle Triassic) of Tanzania and its implications for body-
400 size evolution in Dinosauromorpha: Gondwana Research, v. 27, p. 925-931.
401 Benton, M. J., and Newell, A. J., 2014, Impacts of global warming on Permo-Triassic terrestrial
402 ecosystems: Gondwana Research, v. 25, p. 1308-1337.
403 Butler, R. J., Barrett, P. M., Abel, R. L., and Gower, D. J. 2009. A possible ctenosauriscid
404 archosaur from the Middle Triassic Manda Beds of Tanzania: Journal of Vertebrate
405 Paleontology, v. 29, no. 4, p. 1022-1031.
406 Butler, R. J., Nesbitt, S. J., Charig, A. J., Gower, D. J., and Barrett, P. M., 2017, *Mandasuchus*
407 *tanyauchen*, gen. et sp. nov., a pseudosuchian archosaur from the Manda Beds (?Middle
408 Triassic) of Tanzania: Journal of Vertebrate Paleontology, v. 37, no. sup1, p. 96-121.
409 Butler, R. J., Jones, A. S., Buffetaut, E., Mandl, G. W., Scheyer, T. M., and Schultz, O. 2019.
410 Description and phylogenetic placement of a new marine species of phytosaur
411 (Archosauriformes: Phytosauria) from the Late Triassic of Austria: Zoological Journal of
412 the Linnean Society, zlz014, https://doi.org/10.1093/zoolinnean/zlz014.
413 Chen, Z.-Q., and Benton, M. J., 2012, The timing and pattern of biotic recovery following the
414 end-Permian mass extinction: Nature Geoscience, v. 5, p. 375.

415 Ciampaglio, C.N., Kemp, M., and McShea, D.W., 2001, Detecting changes in morphospace
416 occupation patterns in the fossil record: characterization and analysis of measures of
417 disparity: Paleobiology, v. 27, p. 695-715.
418 de Oliveira, T. M., and Pinheiro, F. L., 2017, Isolated archosauriform teeth from the Upper
419 Triassic Candelária Sequence (Hyperodapedon Assemblage Zone, Southern Brazil):
420 Revista Brasileira de Paleontologia, v. 20, p. 155-162.
421 Dessem, D. 1985. Ontogenetic changes in the dentition and diet of *Tupinambis* (Lacertilia:
422 Teiidae). Copeia, v. 1985, no. 1, p. 245-247.
423 Dzik, J., 2003, A beaked herbivorous archosaur with dinosaur affinities from the early Late
424 Triassic of Poland: Journal of Vertebrate Paleontology, v. 23, p. 556-574.
425 Erwin, D. H., 1994, The Permo–Triassic extinction: Nature, v. 367, p. 231.
426 Ezcurra, M. D., 2016, The phylogenetic relationships of basal archosauromorphs, with an
427 emphasis on the systematics of proterosuchian archosauriforms: PeerJ, v. 4, p. e1778.
428 Ezcurra, M. D., and Butler, R. J., 2018, The rise of the ruling reptiles and ecosystem recovery
429 from the Permo-Triassic mass extinction: Proc R Soc Lond B Biol Sci, v. 285, no. 1880,
430 p. 20180361.
431 Foth, C., Ezcurra, M. D., Sookias, R. B., Brusatte, S. L., and Butler, R. J., 2016, Unappreciated
432 diversification of stem archosaurs during the Middle Triassic predated the dominance of
433 dinosaurs: BMC Evolutionary Biology, v. 16, no. 1, p. 188.
434 Fraser, N. C., and Walkden, G. M., 1983, The ecology of a Late Triassic reptile assemblage from
435 Gloucestershire, England: Palaeogeography, Palaeoclimatology, Palaeoecology, v. 42, p.
436 341-365.

437 Gavrilets, S., and Losos, J. B., 2009, Adaptive Radiation: Contrasting Theory with Data:
438 Science, v. 323, no. 5915, p. 732-737.
439 Godefroit, P., and Cuny, G. 1997. Archosauriform teeth from the upper Triassic of Saint-
440 Nicolas-de-Port (northeastern France): Palaeovertebrata, 26(1-4), 1-34.
441 Griffin, C. T., and Nesbitt, S. J., 2016, The femoral ontogeny and long bone histology of the
442 Middle Triassic (?late Anisian) dinosauriform *Asilisaurus kongwe* and implications for
443 the growth of early dinosaurs: Journal of Vertebrate Paleontology, v. 36, no. 3.
444 Grossnickle, D. M., and Polly, P. D., 2013, Mammal disparity decreases during the Cretaceous
445 angiosperm radiation: Proceedings of the Royal Society of London B: Biological
446 Sciences, v. 280, no. 1771, p. 20132110.
447 Hammer, Ø., Harper, D., and Ryan, P., 2001, PAST-Palaeontological statistics: Palaeontologia
448 Electronica, v. 25, no. 07, p. 2009.
449 Hendrickx, C., Mateus, O., and Araújo, R. 2015, A proposed terminology of theropod teeth
450 (Dinosauria, Saurischia): Journal of Vertebrate Paleontology, v. 35, no. 5, e982797.
451 Hungerbühler, A., 2000, Heterodonty in the European phytosaur *Nicrosaurus kapffi* and its
452 implications for the taxonomic utility and functional morphology of phytosaur dentitions:
453 Journal of Vertebrate Paleontology, v. 20, p. 31-48.
454 Kubo, T., and Kubo, M. O., 2014, Dental microwear of a Late Triassic dinosauriform, *Silesaurus*
455 *opolensis*: Acta Palaeontologica Polonica, v. 59, p. 305-313.
456 Larson, D. W., 2008, Diversity and variation of theropod dinosaur teeth from the uppermost
457 Santonian Milk River Formation (Upper Cretaceous), Alberta: a quantitative method
458 supporting identification of the oldest dinosaur tooth assemblage in Canada: Canadian
459 Journal of Earth Sciences, v. 45, no. 12, p. 1455-1468.

460 Larson, D. W., and Currie, P. J., 2013, Multivariate analyses of small theropod dinosaur teeth
461 and implications for paleoecological turnover through time: PLoS One, v. 8, no. 1, p.
462 e54329.
463 Larson, D. W., Brown, C. M., and Evans, D. C., 2016, Dental disparity and ecological stability in
464 bird-like dinosaurs prior to the end-Cretaceous mass extinction: Current Biology, v. 26,
465 no. 10, p. 1325-1333.
466 Lenth, R. V., 2016, Least-Squares Means: The R Package lsmeans. Journal of Statistical
467 Software, v. 69, no. 1, 1-33. doi:10.18637/jss.v069.i01
468 Li, C., Wu, X.-c., Cheng, Y.-n., Sato, T., and Wang, L., 2006, An unusual archosaurian from the
469 marine Triassic of China: Naturwissenschaften, v. 93, no. 4, p. 200-206.
470 Lucas, P.W. 1979. The dental-dietary adaptations of mammals: Neues Jahrbuch für Geologie und
471 Paläontologie, Monatshefte, v. 8, p. 486–512.
472 Linde, M., Palmer, M., and Gómez-Zurita, J. 2004, Differential correlates of diet and phylogeny
473 on the shape of the premaxilla and anterior tooth in sparid fishes (Perciformes: Sparidae):
474 Journal of Evolutionary Biology, v. 17, no. 5, p. 941-952.
475 Marsicano, C. A., Irmis, R. B., Mancuso, A. C., Mundil, R., and Chemale, F., 2016, The precise
476 temporal calibration of dinosaur origins: Proceedings of the National Academy of
477 Sciences, v. 113, no. 3, p. 509-513.
478 Nesbitt, S. J., Sidor, C. A., Irmis, R. B., Angielczyk, K. D., Smith, R. M. H., and Tsuji, L. A.,
479 2010, Ecologically distinct dinosaurian sister group shows early diversification of
480 Ornithodira: Nature, v. 464, p. 95-98.
481 Nesbitt, S. J., 2011, The Early Evolution of Archosaurs: Relationships and the Origin of Major
482 Clades: Bulletin of the American Museum of Natural History, p. 1-292.

483 Nesbitt, S. J., Butler, R. J., and Gower, D. J., 2013, A new archosauriform (Reptilia: Diapsida)
484 from the Manda beds (Middle Triassic) of southwestern Tanzania: PLoS One, v. 8,
485 e72753.
486 Nesbitt, S. J., Sidor, C. A., Angielczyk, K. D., Smith, R. M. H., and Tsuji, L. A., 2014, A new
487 archosaur from the Manda beds (Anisian: Middle Triassic) of southern Tanzania and its
488 implications for character optimizations at Archosauria and Pseudosuchia: Journal of
489 Vertebrate Paleontology, v. 34, p. 1357-1382.
490 Nesbitt, S. J., Butler, R. J., Ezcurra, M. D., Barrett, P. M., Stocker, M. R., Angielczyk, K. D.,
491 Smith, R. M., Sidor, C. A., Niedźwiedzki, G., Sennikov, A. G. and Charig, A. J., 2017,
492 The earliest bird-line archosaurs and the assembly of the dinosaur body plan: Nature, v.
493 544, p. 484-487.
494 Ottone, E. G., Monti, M., Marsicano, C. A., Marcelo, S., Naipauer, M., Armstrong, R., and
495 Mancuso, A. C., 2014, A new Late Triassic age for the Puesto Viejo Group (San Rafael
496 depocenter, Argentina): SHRIMP U–Pb zircon dating and biostratigraphic correlations
497 across southern Gondwana: Journal of South American Earth Sciences, v. 56, p. 186-199.
498 Peecook, B. R., Steyer, J. S., Tabor, N. J., Smith, R. M., 2017, Updated geology and vertebrate
499 paleontology of the Triassic Ntawere Formation of northeastern Zambia, with special
500 emphasis on the archosauromorphs: Journal of Vertebrate Paleontology, 37(sup1), 8-38.
501 Polly, P. D., 2008, Adaptive zones and the pinniped ankle: a three-dimensional quantitative
502 analysis of carnivoran tarsal evolution, Mammalian evolutionary morphology: Dordrecht,
503 Springer, p. 167-196.

504 Qvarnström, M., Wernström, J. V., Piechowski, R., Tałanda, M., Ahlberg, P. E. and
505 Niedźwiedzki, G., 2019, Beetle-bearing coprolites possibly reveal the diet of a Late
506 Triassic dinosauriform: Royal Society Open Science, v. 6, p.181042.
507 Raup, D. M., 1979, Size of the Permo-Triassic bottleneck and its evolutionary implications:
508 Science, v. 206, no. 4415, p. 217-218.
509 Rubidge, B. S., 2005, 27th Du Toit Memorial Lecture: re-uniting lost continents–fossil reptiles
510 from the ancient Karoo and their wanderlust: South African Journal of Geology, v. 108,
511 no. 1, p. 135-172.
512 Sander, P. M., 1997,Teeth and jaws. Encyclopedia of dinosaurs, p. 717-725.
513 Santana, S. E., Strait, S., and Dumont, E. R., 2011, The better to eat you with: functional
514 correlates of tooth structure in bats: Functional Ecology, v. 25, no. 4, p. 839-847.
515 Scanlon, J. D., and Shine, R., 1988, Dentition and diet in snakes: adaptations to oophagy in the
516 Australian elapid genus *Simoselaps*: Journal of Zoology, v. 216, no. 3, p. 519-528.
517 Schluter, D., 1996, Ecological Causes of Adaptive Radiation: The American Naturalist, v. 148,
518 p. S40-S64.
519 Schoch, R. R., Ullmann, F., Rozynek, B., Ziegler, R., Seegis, D., & Sues, H. D., 2018, Tetrapod
520 diversity and palaeoecology in the German Middle Triassic (Lower Keuper) documented
521 by tooth morphotypes: Palaeobiodiversity and Palaeoenvironments, v. 98, p. 615-638.
522 Sidor, C. A., and S. J. Nesbitt., 2017, Introduction to vertebrate and climatic evolution in the
523 Triassic rift basins of Tanzania and Zambia; pp. 1–7 in C. A. Sidor and S. J. Nesbitt
524 (eds.), Vertebrate and Climatic Evolution in the Triassic Rift Basins of Tanzania and
525 Zambia. Society of Vertebrate Paleontology Memoir 17. Journal of Vertebrate
526 Paleontology 37 (6, Supplement).

527 Simpson, G. G., 1944, Tempo and Mode in Evolution, New York, Columbia University Press.
528 -, 1953, Major features of evolution, New York, Columbia University Press.
529 Smith, J. B., Vann, D. R., and Dodson, P., 2005, Dental morphology and variation in theropod
530 dinosaurs: implications for the taxonomic identification of isolated teeth: The Anatomical
531 Record, v. 285, no. 2, p. 699-736.
532 Smith, R. M., Sidor, C. A., Angielczyk, K. D., Nesbitt, S. J., and Tabor, N. J., 2018, Taphonomy
533 and paleoenvironments of Middle Triassic bone accumulations in the Lifua Member of
534 the Manda Beds, Songea Group (Ruhuhu Basin), Tanzania: Journal of Vertebrate
535 Paleontology, v. 37, no. sup1, p. 65-79.
536 Team, R. C., 2018, R: A Language and Environment for Statistical Computing.
537 Turner-Walker, G., 2008, The chemical and microbial degradation of bones and teeth: Advances
538 in human palaeopathology, v. 592.
539 Wickham, H., 2009, ggplot2: elegant graphics for data analysis, New York, Springer.
540 Wynd, B. M., Sidor, C. A., Whitney, M. R., and Peecook, B. R., 2018, The first occurrence of
541 *Cynognathus* in Tanzania and Zambia, with biostratigraphic implications for the age of
542 Triassic strata in southern Pangea. Vertebrate and climatic evolution in the Triassic rift
543 basins of Tanzania and Zambia: Society of Vertebrate Paleontology Memoir, v. 17, p.
544 228-239.
545 Zahradnicek, O., Buchtova, M., Dosedelova, H., and Tucker, A. S., 2014, The development of
546 complex tooth shape in reptiles: Frontiers in Physiology, v. 5, p. 74.
547 Zverkov, N. G., Fischer, V., Madzia, D., and Benson, R. B., 2018, Increased pliosaurid dental
548 disparity across the Jurassic-Cretaceous transition: Palaeontology, v.61, p. 1-22.

Figure 1

A sample of the *in situ* dental material used for baseline measurements in this study.

A – *Parringtonia* (NMT RB426) left dentary (left) in lateral (top) and medial (bottom) views and right dentary (right) in lateral and medial views. B – undescribed archosauriform taxon (NMT RB187) right maxilla in lateral and medial view. C – *Nundasuchus* (NMT RB48) holotype right dentary in lateral and medial views. D – *Asilisaurus* (NMT RB 837) (from left to right) right dentary in lateral and medial views, left maxilla in lateral and occlusal views, and right maxilla in lateral and occlusal views. Abbreviations: ap, ascending process of the maxilla; ds, dentary symphysis; ga, gastralia; mg, Meckelian groove; mt III, metatarsal III; nf, nutrient foramen; pp, palatal process. All scale bars 1 cm.

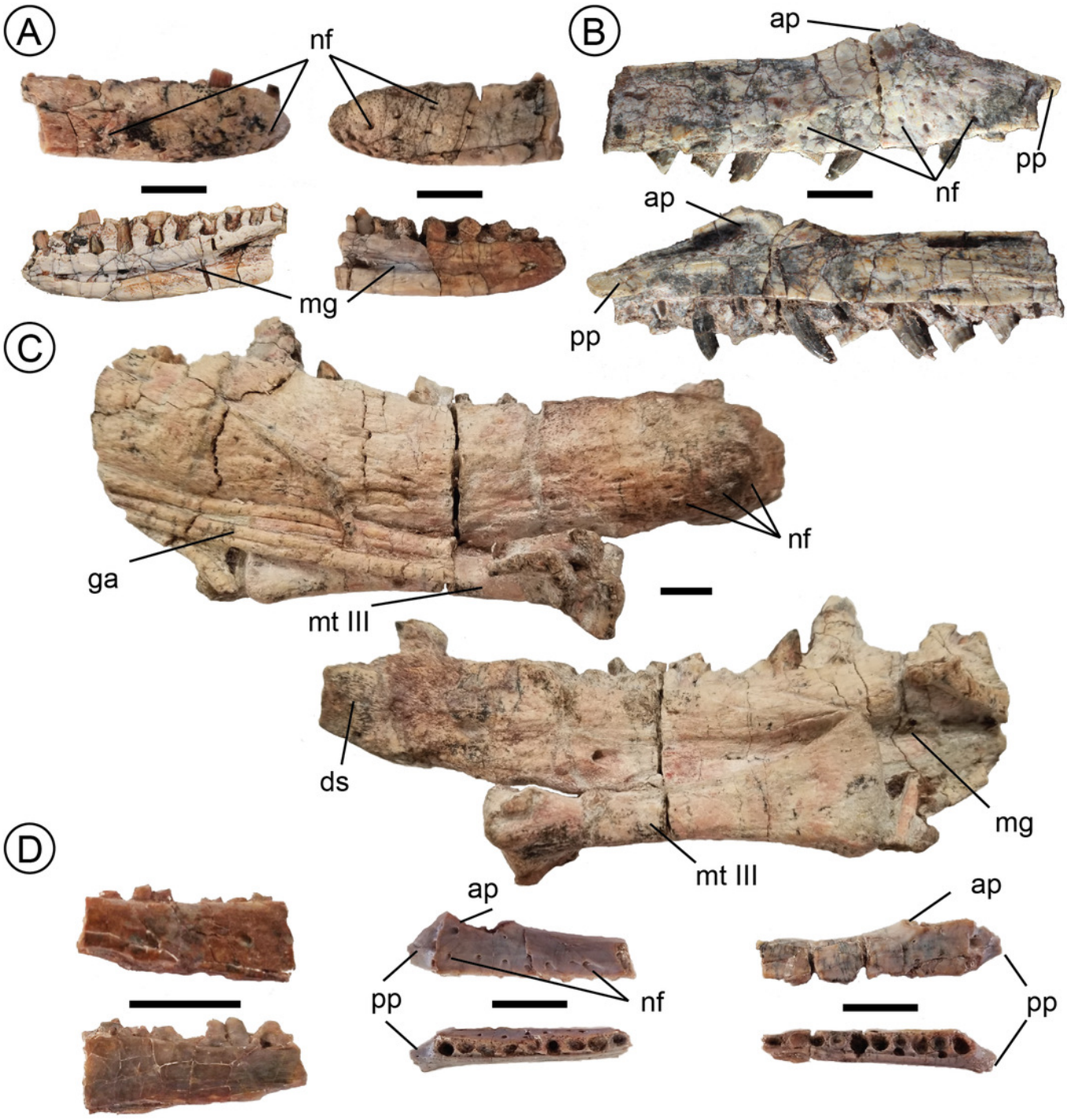
A
nf
mg
B
ap
pp
nf
ap
pp
C
ga
nf
mt III
ds
mg
mt III
D
ap
pp
nf
ap
pp

Figure 2

Examples of isolated teeth from the Manda Beds tooth assemblage.

A – Morphotype A specimens from left to right NMT RB807, NMT RB827, NMT RB809 in lateral and mesial views. Scale bars 1 cm. B – Morphotype B, specimens from left to right, NMT RB810, NMT RB819, NMT RB811 in lateral and mesial views. Scale bars 5 mm. C – sole representative of Morphotype C NMT RB831 in lateral and mesial views. Scale bar 1 cm. D – isolated teeth of known taxa. Top – *Nundasuchus* NMT RB48. Scale bar 1 cm. Bottom – *Parringtonia* NMT RB426 in lateral and mesial views. Scale bar 2 mm.


A
B
C
D

Figure 3

Visualization of discrete traits.

In all traits score 0 on left and score 1 on right. A – Trait 1, degree of recurvature, NMT RB819 (left) and NMT RB827 (right). B – Trait 2, fluting, NMT RB809 (left) and NMT RB426 (right). C – Trait 3, labiolingual curvature, NMT RB811 (left) and NMT RB819 (right). D – Trait 4, mesial margin angle, NMT RB811 (left) and NMT RB827 (right). E – Trait 5, labiolingual bulge, NMT RB811 (left) and NMT RB48 (right). F – Trait 6, dental caudae, NMT RB809 (left) and NMT RB810 (right). G – Trait 7, mesial vs distal serration series length, NMT RB831 (left) and NMT RB810 (right). H – Trait 8, denticle density per mm, NMT RB809 (left) and NMT RB810 (right), black lines equal 1 mm. I – Trait 9, mesial margin alignment, NMT RB810 (left) and NMT RB809 (right). J – Trait 10, mesial vs distal denticle density, NMT RB810 (left) and NMT RB809 (right). K – Trait 11, denticle shape variation along crown, NMT RB810 (left) and NMT RB48 (right).

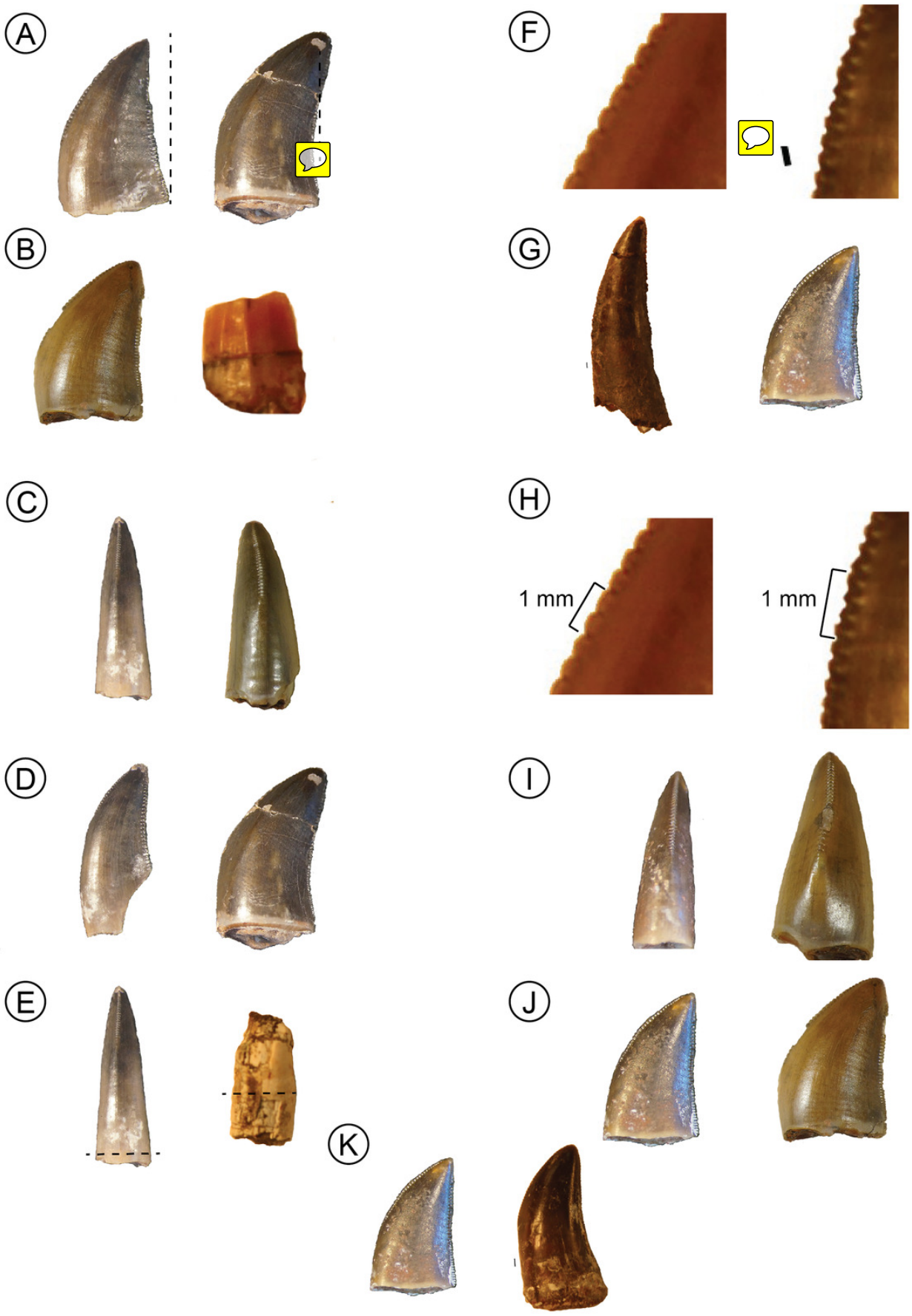
A
B
C
D
E
K
F
G
H
1 mm
1 mm
I
J

Figure 4(on next page)

Disparity of teeth measured by sum of variance

Disparity divided by taxon or morphotype. In the case of *Parringtonia* the two isolated teeth are an order of magnitude larger than the *in situ* teeth of this taxon, so this taxon was split. The sample sizes reflect the number of teeth with at least one of three measurements that was used to generate the predictive intervals.

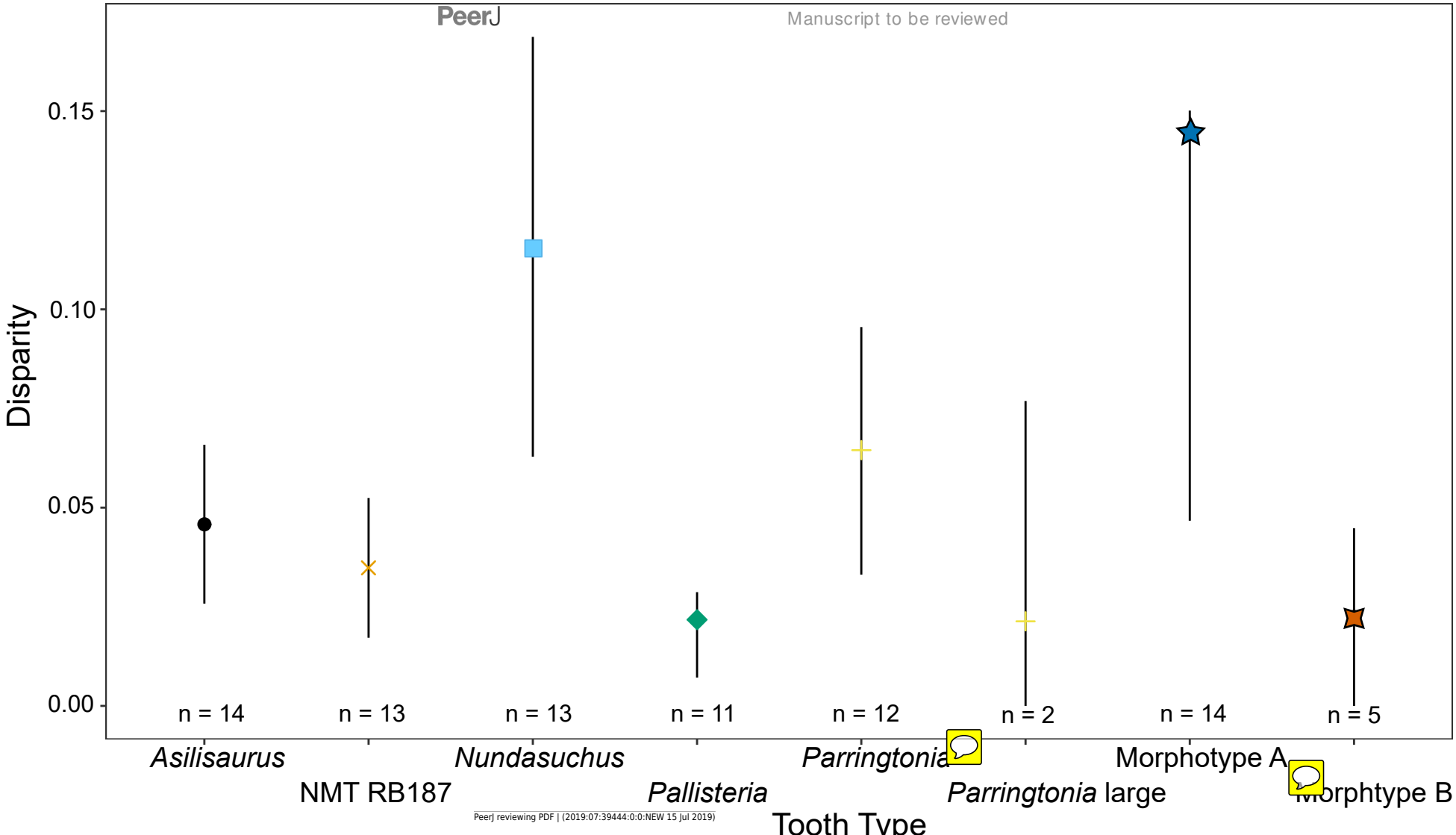
Disparity
0.15
0.10
0.05
0.00
n = 14
n = 13
n = 13
n = 11
n = 12
n = 2
n = 14
n = 5
Asilisaurus
NMT RB187
Nundasuchus
Pallisteria
Parringtonia
Parringtonia large
Morphotype A
Morphtype B
Tooth Type

Figure 5(on next page)

Relationship between height and base shape of teeth divided by taxon.

The taxonomically unidentified teeth fall within a variety of the morphospaces generated by known taxa, rendering unambiguous referrals impossible. Some genera exhibit much greater variation in base shape ratio than others, potentially indicating a greater level of within-taxon variation.

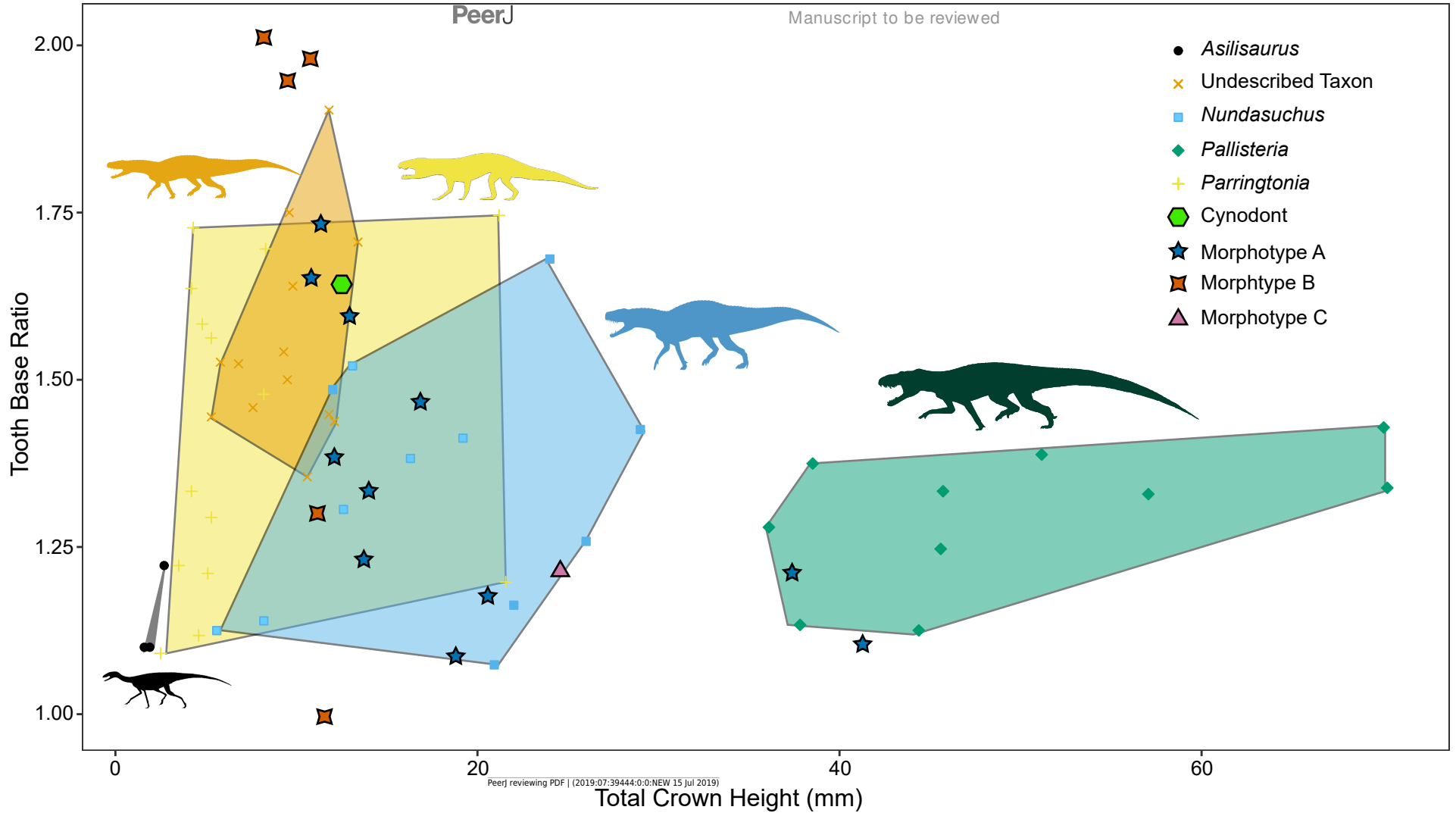
Asilisaurus
Undescribed Taxon
Nundasuchus
Pallisteria
Parringtonia
Cynodont
Morphotype A
Morphtype B
Morphotype C
Tooth Base Ratio
2.00
1.75
1.50
1.25
1.00
0
20
40
60
Total Crown Height (mm)

Figure 6(on next page)

Relationship between base width and fore-aft base length divided by taxon.

The overall ratio of base shape appears to be highly conserved with little deviation from the general trend. Differentiation between genera appears to be driven primarily by size.

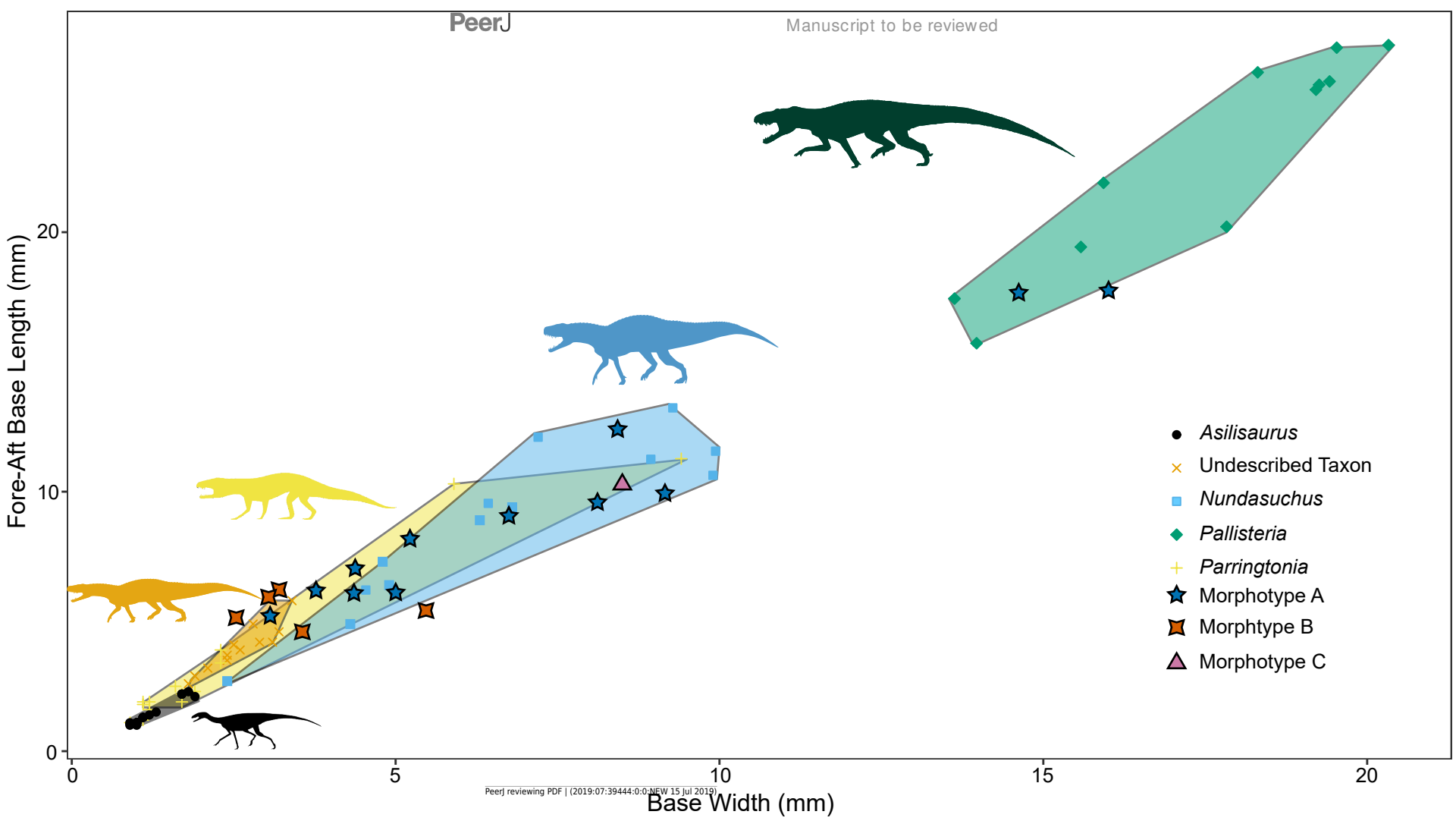
Fore-Aft Base Length (mm)
0
10
20
0
5
10
15
20
Base Width (mm)
Asilisaurus
Undescribed Taxon
Nundasuchus
Pallisteria
Parringtonia
Morphotype A
Morphtype B
Morphotype C

Figure 7 (on next page)

Ordination plot of first two major NMDS axes of tooth morphospace.

Colored, transparent polygons represent the convex hulls of known taxa. Each point represents a separate tooth scoring. *Parringtonia* and NMT RB187 (undescribed taxon) share almost the same morphospace and there is substantial overlap between *Nundasuchus* and '*Pallisteria*' also. Morphotype A appears to be more variable than Morphotype B, which is clustered closer together within a subsection of overall Morphotype A morphospace. The proximity of *Asilisaurus* to *Nundasuchus* and '*Pallisteria*' is likely an artifact of incomplete scorings for *Asilisaurus* teeth.

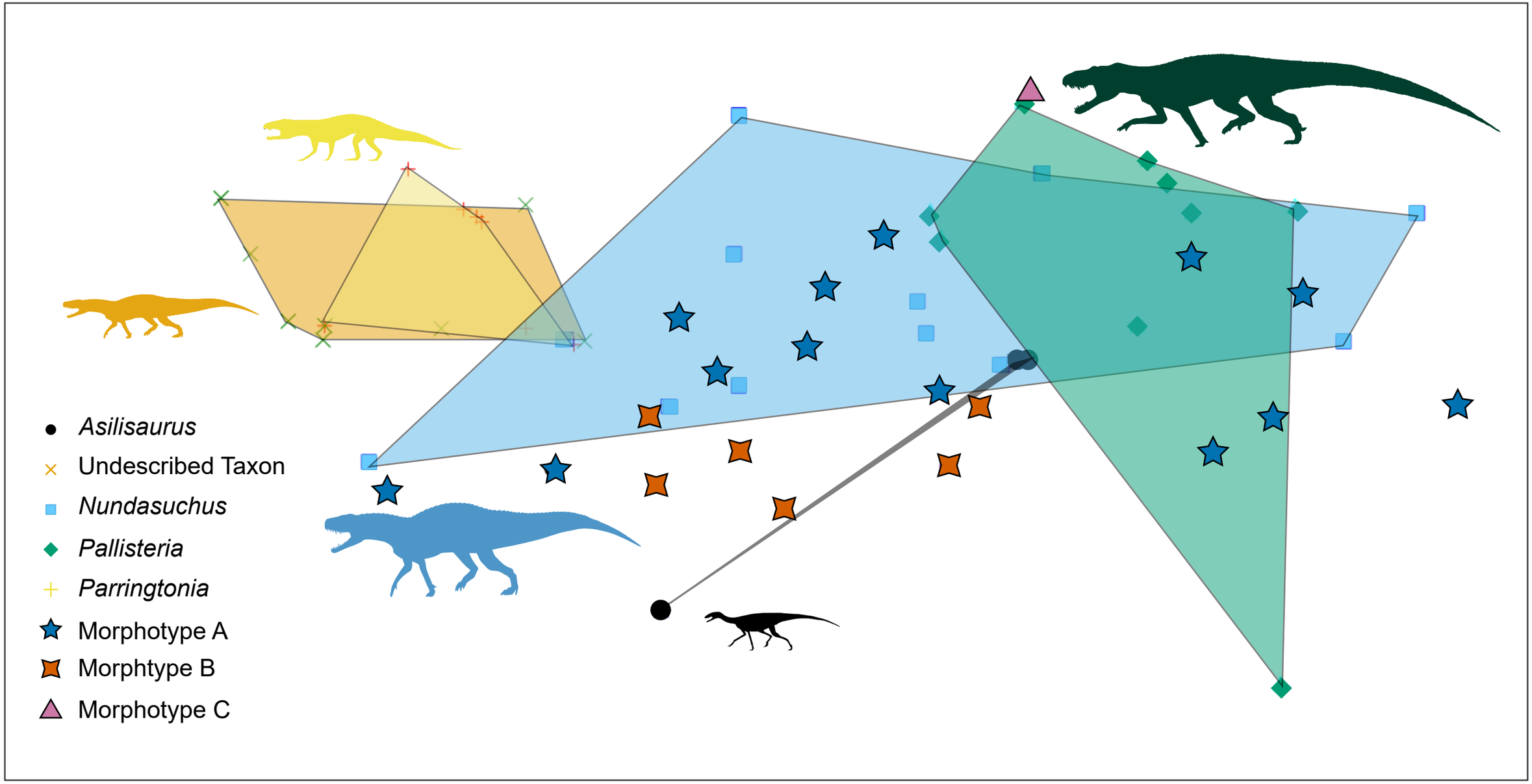
NMDS 2
NMDS 1
Asilisaurus
Undescribed Taxon
Nundasuchus
Pallisteria
Parringtonia
Morphotype A
Morphtype B
Morphotype C

Figure 8(on next page)

Ordination plot of first two primary NMDS axes of tooth "averages" morphospace.

Taxa scoring represent “average” scores for each taxon. Only Morphotype C is represented by a single tooth. When using typical scores for taxa we find *Asilisaurus* is no longer near *Nundasuchus* and ‘*Pallisteria*’ morphospace, but on the far side of ordination space.

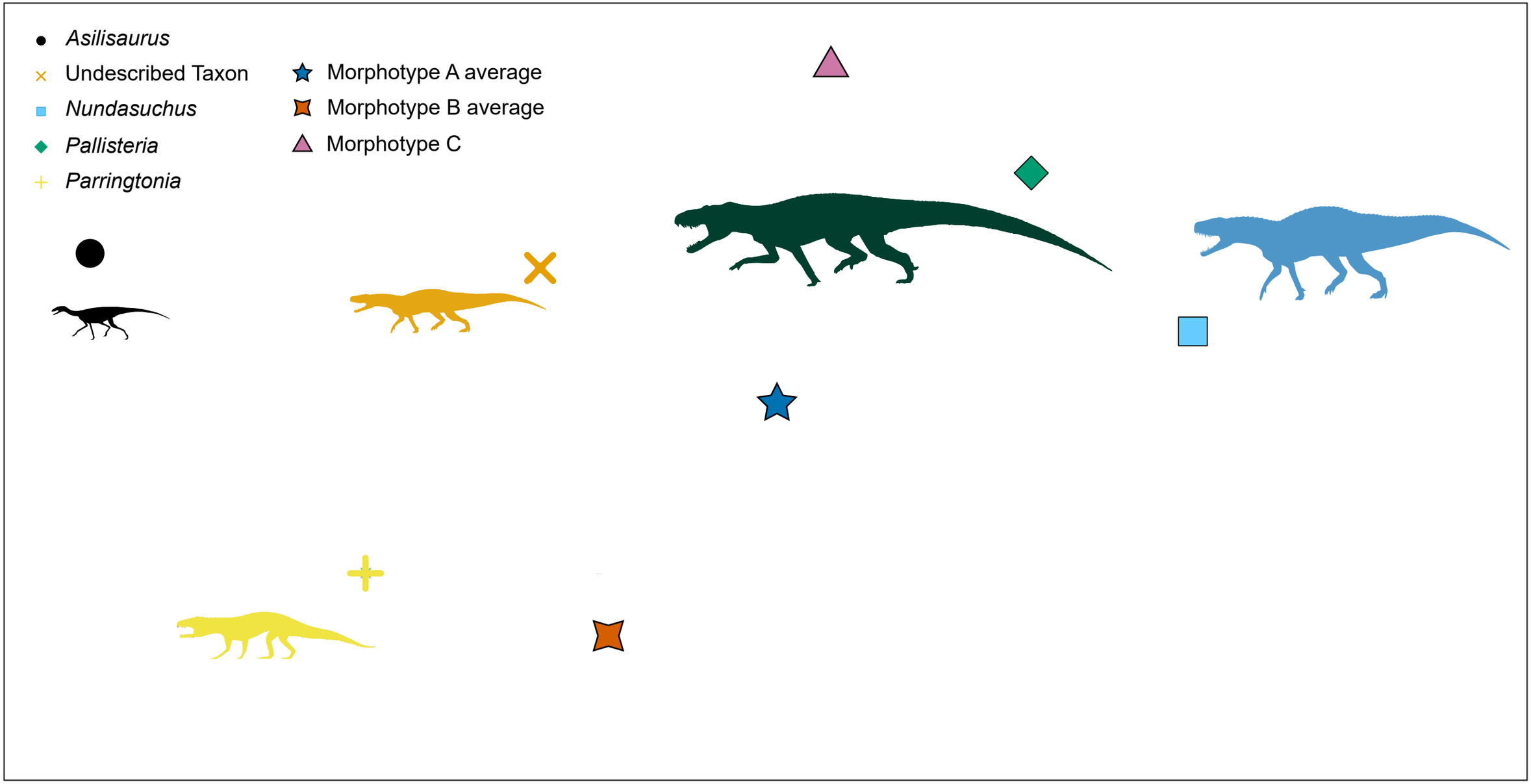
Asilisaurus
Undescribed Taxon
Nundasuchus
Pallisteria
Parringtonia
Morphotype A average
Morphotype B average
Morphotype C
NMDS 2
NMDS 1

Table 1(on next page)

Discrete character descriptions

Summary of the discrete, binary traits used for scoring teeth in the NMDS analysis.

	Description
1	Tooth apex, location, relative to the distal margin of the tooth base: tip mesial to or in the same vertical plane as the distal edge (0) or tip is located more distal than the distal edge (=recurved) (1)
2	Tooth lingual/labial, surfaces: texture is smooth (lack of crenulations, ridges, etc.) (0) or surface texture possess a series of parallel ridges from tooth apex to base (=fluted) (1)
3	Tooth labial/lingual, shape: crown curvature unequal (one side expanded relative to other) (0) or equal labial and lingual curvature (1)
4	Mesial tooth margin, shape: curvature angles change gradually (0) or angle changes abruptly at a single discrete point along mesial edge (1)
5	Tooth crown, size: labiolingual widths dorsal to the tooth crown base are all less than the crown base width (0) or a crown labiolingual width dorsal to the tooth crown base is greater than the crown base width (1)
6	Mesial/distal crown margins, surfaces: denticle caudae (= grooves on crown surface from between individual denticles) are absent (0) or present (1) (from Abler, 1992)
7	Mesial margin, length: mesial denticle row ends at a point sub-equal with distal denticle row (0) or mesial denticle row ends significantly further apically on crown than distal row (1). Can only be scored for teeth with both mesial and distal denticle series.
8	Mesial/distal margins, denticle density: number of mesial and distal denticles is < 3 per mm (0), or greater than or equal to 3 per mm (1). Measurements are taken near the middle of the carina.
9	Mesial margin, location: vertical axis of the mesial carina is in line the mesial-distal long axis (0) or laterally offset from the mesial distal long axis (1)
10	Mesial/distal margins, size: average size of mesial and distal denticles are the same (0) or the average size of the mesial and distal denticles is different (1)
11	Mesial/distal margins, shape: lateral profile shape of mesial and distal denticles remains constant (0) or denticles' lateral profile changes shape (e.g. rounded to square) (1)

1

Table 2(on next page)

Results of linear model (base ~ total crown height + taxon)

All measures of significance are calculated in reference to the intercept, *Asilisaurus*. Therefore, while the undescribed pseudosuchian and *Parringtonia* can be differentiated in the model from *Asilisaurus*, the interrelationships are unknown.

	Estimate	Standard Error	t-value	p-value
Asilisaurus (intercept)	1.1285	0.1011	11.156	<0.0001
Total Crown Height (mm)	0.0059	0.0035	1.714	0.0933
Undescribed	0.3718	0.1148	3.237	0.0022
Nundasuchus	0.0995	0.1247	0.798	0.4290
'Pallisteria'	-0.1249	0.2007	-0.622	0.5369
Parringtonia	0.2490	0.1127	2.210	0.0321

1

Table 3(on next page)

Pairwise comparisons of taxa used in the linear model.

The undescribed pseudosuchian is readily differentiable from most taxa, with the exception of *Parringtonia*. Confidence intervals were generated using a 95% confidence level.

Taxon	lsmeans	Standard Error	df	Lower CL	Upper CL
Asilisaurus	1.2354	0.1150	46	1.0039	1.4669
Undescribed	1.6071	0.0568	46	1.4929	1.7214
Nundasuchus	1.3348	0.0505	46	1.2332	1.4365
'Pallisteria'	1.1105	0.1225	46	0.8640	1.3570
Parringtonia	1.4844	0.0595	46	1.3645	1.6042

1

Contrast	Estimate	SE	df	t ratio	p-value
Asilisaurus – Undescribed	-0.3718	0.1148	46	-3.237	0.0181
Asilisaurus – Nundasuchus	-0.0995	0.1247	46	-0.798	0.9299
Asilisaurus – 'Pallisteria'	0.1249	0.2007	46	0.622	0.9708
Asilisaurus – Parringtonia	-0.2490	0.1127	46	-2.210	0.1944
Undescribed – *Nundasuchus*	0.2723	0.0751	46	3.625	0.0062
Undescribed – *'Pallisteria'*	0.4967	0.1571	46	3.162	0.0222
Undescribed – *Parringtonia*	0.1228	0.0677	46	1.813	0.3788
Nundasuchus – 'Pallisteria'	0.2244	0.1343	46	1.671	0.4614
Nundasuchus – Parringtonia	-0.1495	0.0770	46	-1.942	0.3107
'Pallisteria' – Parringtonia	-0.3739	0.1631	46	-2.292	0.1659

2